Charge Transfer and OH Vibrational Frequency Red Shifts in Nitrate−Water Clusters

Sai G. Ramesh[†] and Suyong Re[‡]

Département de Chimie, UMR 8640 PASTEUR, École Normale Supérieure, 24 rue Lhomond, 75231 Paris CEDEX 05, France

James T. Hynes*

Département de Chimie, UMR 8640 PASTEUR, École Normale Supérieure, 24 rue Lhomond, 75231 Paris CEDEX 05, France, and Department of Chemistry and Biochemistry, University of Colorado, Boulder, Colorado 80309−0215

Received: July 31, 2007; In Final Form: December 19, 2007

A theoretical study of charge transfer (CT) characteristics in nitrate (NO_3^-) anion−water complexes is presented, together with those for the halides, F^-, Cl^-, and Br^-, for comparison. The relation between the vibrational frequency red shifts of the hydrogen (H)-bonded OH stretches and CT from the anion to the water molecule, established in previous work for the one-water complexes of the halides, is studied for both the one- and six-water nitrate complexes and is extended to the six-water case for the halides. In $NO_3^-\cdot H_2O$, the water molecule receives about as much charge as that in $Br^-\cdot H_2O$. In a result consistent with aqueous phase infrared experiments [Bergström, P. A.; Lindgren, J.; Kristiansson, O. *J. Phys. Chem.* **1991**, *95*, 8575−8580], the CT and OH red shift in $NO_3^-\cdot 6H_2O$ are found to be smaller than those for all of the six-water halide complexes, despite the presence of three H-bonding sites. The inability of the nitrate anion to effect substantial CT lies in the preservation of the π-system being energetically favored over charge localization and enhancement of the strengths of the multiple H-bonds.

1. Introduction

The nitrate ion, NO_3^-, is of interest in a wide variety of contexts. In the area of atmospheric chemistry, NO_3^--containing nitrate aerosols represent one type of heterogeneous reaction site in connection with ozone depletion in the stratosphere,[1] and NO_3^- is a reaction product of some of the key heterogeneous reactions in this region.[1,2] Largely in connection with its role as a potential product of nitric acid HNO_3 dissociation in aerosol surface regions, NO_3^- is also important in other atmospheric regions, such as the upper troposphere[3] and the marine troposphere,[4] where it plays a role in the removal or regeneration of NO_x species in the atmosphere. Accordingly, surface-sensitive vibrational spectroscopic[5] and other[6] experiments have been concerned with NO_3^- detection, and theoretical investigations have been carried out both of NO_3^- production via nitric acid dissociation at aqueous surfaces[7] and of the spatial distribution of NO_3^- at such surfaces.[8] The comprehension of OH stretch frequency shifts for water molecules solvating the nitrate anion in such situations is clearly of interest in connection with spectroscopic experiments probing these issues.

Of course, the nitrate anion has also long been of interest in bulk aqueous solution. Using its vibrations as a probe, several infrared (IR) and Raman investigations have been carried out to study contact and solvent-separated ion-pair formation in solution.[9] These studies revealed a sizable influence of both the cation and the concentration on the spectral bands of NO_3^-. A feature of special interest in these studies, and revived in recent years,[10,11] has been the issue of "symmetry breaking" in the anion in solution. This is experimentally visible as the solvent-induced spectroscopic splitting of the antisymmetric NO stretching vibrations of the isolated D_{3h} anion.[6,9,10,12]

The advent of ultrafast infrared spectroscopic techniques has opened a new window on the dynamics of water molecules hydrogen (H)-bonded to anions in solution via OH stretch probing.[13−15] For molecular anions, the vibrational dynamics of the anions themselves in such H-bonded situations may also be investigated. Given its widespread importance, NO_3^- represents an important future target for such experiments.

In view of the preceding, attention is merited to the fundamental issues of (a) the character of the NO_3^-−H_2O H-bond, (b) its influence on the frequency of the OH stretch involved in the H-bond, and of the (c) electronic and (d) vibrational characters of the NO_3^- anion in an aqueous environment. In this contribution, we present an electronic structure study of the first three of these issues, with the fourth (including vibrational symmetry breaking) to be addressed in a separate study. Of particular concern are the degree and extent of the charge transfer (CT) involved in the NO_3^-−H_2O H-bond − an aspect previously pursued for monatomic halide ion−water dimers, both experimentally[16−18] and theoretically,[18,19] in connection with the OH stretch vibrational frequency red shift (from its value for isolated H_2O) − and the influence of further hydration on both the CT and the OH red shift. A qualitative valence bond perspective, focused on the charge-localizing influence of the anion−water H-bonding (which would assist in increasing CT) in competition with the π-delocalization within the anion (which would tend to resist CT), will be presented to

* To whom correspondence should be addressed. E-mail: hynes@spot.colorado.edu or hynes@chimic.ens.fr.
† E-mail: ramesh@chimie.ens.fr.
‡ E-mail: suyongre@gmail.com.

10.1021/jp0761012 CCC: $40.75
Published on Web 03/20/2008

help frame the analysis of whether the polyatomic nature of N O_3^- could lead to qualitative differences between it and the halide anions in an aqueous solution environment. The outline of the remainder of this paper is as follows. Section 2 is devoted to the methodology employed. The 1:1 nitrate−water complex is studied in section 3, while section 4 is concerned with further solvation of the anion by up to six waters. In both of these sections, the corresponding situations for the halide anions (except for I^-) are included for perspective. Concluding remarks are offered in section 5.

2. Methodology

All ab initio calculations reported in this paper have been carried out using the Gaussian 03 program package.[20] The structures for the $NO_3^-{\cdot}nH_2O$ (n = 1, 2, 4, 6) complexes were obtained at the second-order Møller−Plesset (MP2) level of theory using the augmented correlation-consistent polarized valence double-ζ (aug-cc-pVDZ) basis set.[21] This level of theory has been shown to provide reliable results for the structures and frequencies of H-bonded clusters including anions.[22−24] For comparison, the structures for the corresponding complexes with halide ions, $X^-{\cdot}H_2O$ and $X^-{\cdot}6H_2O$, X = F, Cl, and Br, were also obtained at the same level of theory. Since relativistic effects are not negligible for I^-, iodide−water complexes have been omitted from this work.[25] Most of the structures were optimized with certain constraints (detailed within), and are thus not necessarily stationary points.

Energetics reported within have been corrected for the basis set superposition error (BSSE) by using the counterpoise method.[26] The CT nature of the H-bonds in the nitrate−water and halide−water complexes was analyzed using the natural population analysis (NPA) and natural bond orbital (NBO) schemes of Weinhold and co-workers.[27,28] The red shift of the $\upsilon = 0 \rightarrow 1$ vibrational transition frequency of the H-bonded OH of the H_2O has been calculated by using a one-dimensional sinc-function discrete variable representation (DVR), in which the anharmonicity is fully taken into account.[29,30]

3. One-Water Complexes

3.1. Background. Experimental and theoretical investigations in the past decade on the charge transfer in one-water complexes of monatomic and diatomic anions, particularly the halides, have demonstrated its intimate connection to the magnitudes of the vibrational red shifts of the H-bonded OH stretches.[16−19] CT from the filled lone pair orbitals of ions to the σ^*_{OH} orbital of a partner OH stretch leads to the lengthening of the OH bond as well as the red shift in its transition frequency, the latter being the experimental measure for the overall process.[31,32] Ayotte et al. have reported the OH red shifts for the halide−water heterodimers, and hence the extent of CT in them, to be in the order $I^- < Br^- < Cl^- < F^-$.[16] In terms of the Mulliken picture of proton transfer, the 1:1 complexes can be considered as an intermediate between the limiting $A^- + H_2O$ (reactant) and AH + OH^- (proton-transfer product) structures, where A^- denotes the anion.[33] The product state is produced from the reactant state by CT from the nonbonding orbital on the anion to the σ^*_{OH} orbital.[19,33] Using this pair of states as the basis, Thompson and Hynes have shown that the sizes of the red shifts are much reduced when CT is disallowed.[19] The experimental-cum-theoretical study by Robertson et al. has corroborated this view with an ingenious example of the $^3NO{\cdot}H_2O$ complex in which the CT is spin-suppressed.[17] This leads to a strong OH red-shift diminution compared to that expected based on a red shift versus proton affinity trend shown by the other 1:1 complexes. More recently, it was found that other parts of the vibrational spectrum of these complexes also show strong CT-induced effects.[18]

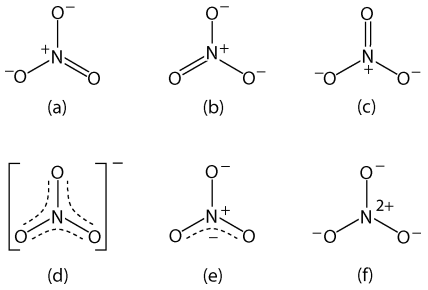

Figure 1. Valence bond structures for NO_3^-. The isolated anion is, of course, a hybrid of the forms (a)−(c), shown as (d). Structure (e) is a limiting situation of charge localization on a single O due to H-bonding with waters on that O. Structure (f) is a limiting situation where charge is localized on all three oxygens due to H-bonding with waters on each of them.

The nitrate−water heterodimers provide an interesting contrast to the above complexes by virtue of the anion's polyatomic nature. One immediate difference is the fact that there are several possible relative orientations of the monomers. The aspect of special import, though, is the effect of H-bonding with water on the resonance hybrid Figure 1d of NO_3^-, arising from the three classic charge-localized valence bond (VB) structures in Figure 1a−c. In a heterodimer, these VB structures will not have an equal weight; from the point of view of the solvating water, a localized charge on the anion's H-bonded O would be favored. To take an extreme view, if the water H-bonding on a particular O were sufficient to localize the charge on that O, a structure like Figure 1e would result, that is, a resonance hybrid of VB structures in Figure 1a and b. This O would then act analogously to a monatomic fully negatively charged halide ion vis-à-vis CT. However, this charge localization would have to occur at the expense of the stabilizing π-delocalization in Figure 1d compared to Figure 1e. If, on the other hand, Figure 1d remains the essentially correct structure of NO_3^- even in the presence of a solvating water, then the charge on the H-bonded O of the nitrate will be noticeably less than unity. The CT to the H-bonded water would be expected to be relatively impeded, perhaps attaining a value smaller than those for the heavy halide ions. These limiting perspectives will prove useful in the interpretation of the electronic structure calculations on N $O_3^-{\cdot}H_2O$ complexes now presented. The obtained data pertaining to CT will also be used as reference for the larger nitrate−water clusters in section 4.

3.2. Structural Details. As noted in the previous subsection, the water molecule in $NO_3^-{\cdot}H_2O$ can be placed around the anion in multiple relative orientations. We have used three singly H-bonded structures in this work, labeled N1, N2, and N3, as shown in Figure 2.[34] The water molecule is out-of-plane with respect to the anion in N1, lying on a vertical bisector plane of NO_3^-, while it is in-plane in the other two structures. The specific spatial placement of the waters in these structures was achieved with constraints that restricted the H_2O's to the aforementioned planes.[35] N3 is the most stable structure of the trio, followed by N2, which is about 3 kcal/mol less stable, results consistent with the findings of Ebner et al. based on an extensive search.[36] N1 has a binding energy smaller by about 4 kcal/mol than that of N3. It is a first-order saddle point[37] and has, perhaps for this reason, not been previously reported. We use N1 in this work withal for it acts as a reference structure in

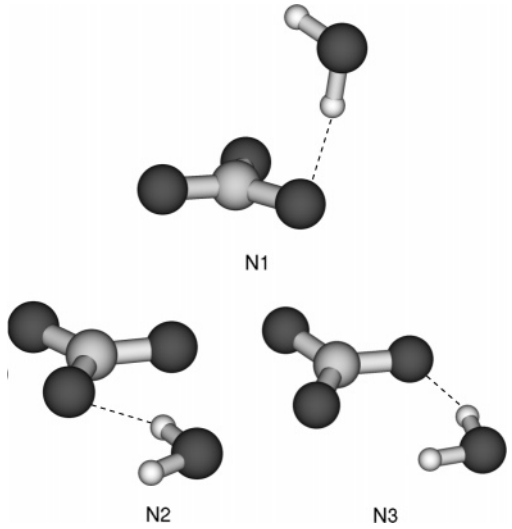

Figure 2. Structures of three $NO_3^-\cdot H_2O$ clusters.

our analyses. In particular, its water molecule and those of the larger $NO_3^-\cdot nH_2O$, $n > 1$, clusters of section 4 are oriented in the same manner relative to the anion. Per water CT properties of these complexes can thus be directly compared as a function of *n*. Various properties computed for N1, N2, and N3 are given in Table 1, along with those for optimized halide−water heterodimers and the water dimer included for comparison.

3.3. Hydrogen-Bonding Characteristics and Relative Placement of NO_3^-. In Figure 3, we plot the OH stretch red shift ($\Delta\nu_{OH}$) for the three $NO_3^-\cdot H_2O$'s and the $X^-\cdot H_2O$'s, X = F, Cl, Br, and I, as a function of the experimental proton affinities (PAs).[17,38] This provides a means of placing the nitrate−water against halide−water heterodimers in terms of the relative H-bond interaction strengths. I^- has been included for completeness in just this one comparison, taking both the experimental $\Delta\nu_{OH}$ and PA data from Robertson et al.[17] NO_3^- does not appear as an exception in the plot; rather, it falls in the trend of the halides, and is positioned around Br^-.

The effects of CT can be analyzed using the natural charge on the water molecule (q_w) (complementary, that on the anion, q_A), the population of the antibonding σ^*_{OH} natural orbital of the H-bonded OH (p^*_{OH}), and its bond length extension (Δr_{OH}). The values of these variables, listed in Table 1, once again show that NO_3^- is not a strong charge donor. Further insight is gained through the correlation plots displayed in Figure 4, where the above variables are plotted against the OH red shift and also against each other. Straight line fits shown in the plots were obtained through the data for only $Cl^-\cdot H_2O$, $Br^-\cdot H_2O$, and N1. The linearity of the $\Delta r_{OH}-\Delta\nu_{OH}$ plot clearly extends up to $F^-\cdot H_2O$ in Figure 4a, showing that OH bond length extension is a faithful indicator of the red shift magnitude.[31] Figure 4b and c utilizes q_w and p^*_{OH}, which are more direct indicators of CT in a H-bonding system. (Recall that the CT is from the nonbonding orbital of the anion to the antibonding orbital of the OH.) Indeed, the correlation plot of these two variables in Figure 4c shows that — at least for complexes of low or moderate H-bond strength, including $NO_3^-\cdot H_2O$ — the transferred charge density mainly appears in the σ^*_{OH} orbital of the H-bonded OH. While the relation of both q_w and p^*_{OH} to $\Delta\nu_{OH}$ is evidently nonlinear, the plots between them echo the conclusions of ref 19 on the importance of the CT in the red shift magnitude. In all three plots of Figure 4, the NO_3^- anion is in line with the halides, with no palpable special CT behavior.

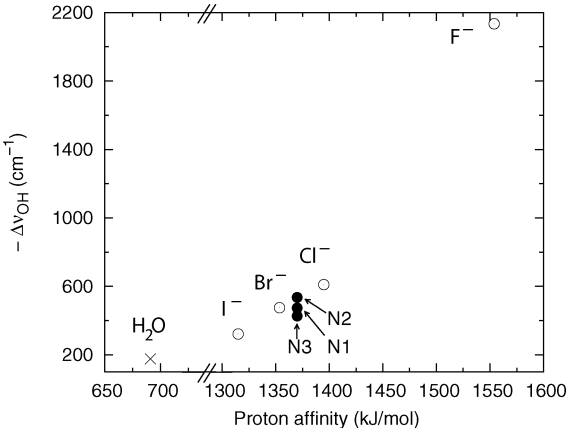

Figure 3. Plot of computed OH stretch red shift versus experimental proton affinity for anion−water 1:1 complexes. The data for I^- were taken from ref 17. All proton affinities were taken from the NIST database.[38,53] The open circles represent the halides, placed in the order I^-, Br^-, Cl^-, and F^- with increasing *x*-coordinate. The filled circles indicate the three nitrate complexes of Figure 2, while the × locates the water dimer. Note the break in the abscissa.

We now address the issue of possible charge localization in NO_3^- broached in section 3.1. The computed charge changes for all of the atoms with respect to the isolated anion are small for all three $NO_3^-\cdot H_2O$'s. For example, the q_O for the donor oxygen of N1 changes from $-0.5578e$ to $-0.5886e$, or by $-0.031e$, while those on the other two O's become less negative by about the same amount. Clearly, the full resonance hybrid of NO_3^- Figure 1d is not broken to produce charge-localized Figure 1e on account of a single H-bond. Supporting this result is the fact that the donor NO bond extends by only 0.012Å compared to its gas-phase length of about 1.269Å. Thus, the H-bond merely acts as a perturbation to the charge distribution of the anion; retention of the π-delocalization is much more important than the gain in H-bonding resulting from the charge localization on the H-bonded NO_3^- oxygen.

It is interesting that the even with only a partial negative charge, the NO_3^- oxygen is able to effect sufficient CT to be ranked with the halides, albeit at the weak, Br^- end of the series. Despite a full −1 charge, the heavy halides are perhaps restricted in their ability to transfer charge owing to a poor overlap of their diffuse charge cloud (4p for Br^-) with the water's σ^*_{OH} orbital. The tighter (2p) donor orbitals of NO_3^- would be expected to overlap more strongly, though short of overall charge.[39] Some amelioration of the charge shortage is probably provided through the π -delocalization; we find that $|q_O|$ for the non-H-bonded NO_3^- oxygens decrease in the main by a sizable 5−7%.

4. *n*-Water Complexes

4.1. Objectives and Choice of Structural Motif. Having found that the resonance hybrid of NO_3^- (Figure 1d) is only weakly perturbed by a single H-bond, we pose the question of whether multiple H-bonding significantly lessens the π-resonance in favor of charge localization on the NO_3^- oxygens, thus enhancing H-bonding with the water molecules. Considering limiting situations, as was done in section 3.1 for the heterodimer, if one or more waters were H-bonded to each of two of the NO_3^- oxygens, a doubly charged-localized VB structure like one of Figure 1a−c could be produced. If one or more waters were H-bonded to each of the three NO_3^- oxygens, the limiting structure Figure 1f could be produced. In both

TABLE 1: Several Properties Computed for One- and Six-Water Clusters of the Anions, as Well as Those for a Reference Water Dimer, *A* and A_d Denoting an Anion and the Donor Site of an Anion, Respectively[a]

complex	$r(A_d-O_w)$ (Å)	Δr_{OH} (Å)	q_A (*e*)	q_w (*e*)	p^*_{OH} (*e*)	$\Delta\nu_{OH}$ (cm^{-1})	$\Delta\nu^{exp}_{OH}$ (cm^{-1})
$(H_2O)_2$	2.9166	0.0069	0.0186	−0.0186	0.0119	−175	
$NO_3^-\cdot H_2O$ (N1)	2.7980	0.0196	−0.9616	−0.0384	0.0253	−472	
$NO_3^-\cdot H_2O$ (N2)	2.7785	0.0234	−0.9540	−0.0460	0.0263	−534	
$NO_3^-\cdot H_2O$ (N3)	2.8131	0.0185	−0.9521	−0.0479	0.0235	−427	
$Br^-\cdot HO$	3.3324	0.0209	−0.9502	−0.0498	0.0303	−474	−437[b]
$Cl^-\cdot H_2O$	3.1365	0.0263	−0.9397	−0.0603	0.0382	−611	−577[b]
$F^-\cdot H_2O$	2.4696	0.0903	−0.8781	−0.1219	0.0880	−2134	
$NO_3^-\cdot 6H_2O$	2.9232	0.0091	−0.9040	−0.0160	0.0117	−214	−181[c]
$Br^-\cdot 6H_2O$	3.4540	0.0106	−0.8608	−0.0232	0.0147	−237	−235[c]
$Cl^-\cdot 6H_2O$	3.3005	0.0114	−0.8554	−0.0241	0.0157	−256	−271[c]
$F^-\cdot 6H_2O$	2.7975	0.0162	−0.8260	−0.0290	0.0190	−381	−350[c]

[a] The reference OH bond length for gas-phase H_2O at the same level of theory is 0.9659Å. The one-dimensional OH stretch frequencies are reported as red shifts relative to the value of 3712 cm^{-1} obtained for a gas-phase OH stretch. Further details are given in section 2. [b] Ref 16a, reference gas-phase $\nu^{exp}_{OH} = 3707$ cm^{-1}, which is the average of the water symmetric and asymmetric stretch frequencies. [c] On the basis of the solution-phase OD frequencies in ref 40. OD red shifts were computed using $\nu^{exp}_{OD} = 2727$ cm^{-1} (gas phase, ref 38) and then scaled by the H/D mass factor ($\sqrt{\mu_{OD}/\mu_{OH}}$).

of these limiting cases, there would be more charge available from the nitrate O's (two or three oxygen donor sites, respectively) to be transferred to the waters than is available in a singly-charged halide ion. Clearly, this last possibility has an important bearing on the behavior of this polyatomic anion in the aqueous phase. Since each NO_3^- oxygen atom in solution interacts with about a third of the anion's hydration shell, it would result in a larger CT for the nitrate anion than that for the halides.

The spectroscopic manifestation of the above changes would be in the aqueous OH red shifts $\Delta\nu_{OH}$, which would be larger for NO_3^- than those for the halides in the limiting cases discussed. The red shifts are available for all four anions under study from the solution phase double difference IR experiments of Bergström et al.[40] These indicate that the $\Delta\nu_{OH}$ for the nitrate anion is *smaller* than those for all of the halides. (OD frequencies were actually measured, which we have mass-scaled to generate OH red shifts; see Table 1.) Assuming that the measured frequency shifts are indeed attributable to the OHs of the anion-H-bonded waters, this result immediately indicates that in solution, just as for the $NO_3^-\cdot H_2O$ heterodimer case, π-delocalizion in the anion is much more important than the H-bonding interaction with the water molecules. Focused on characterizing and understanding this observed behavior of NO_3^-, we set ourselves two tasks. First, we compare the CT properties against those of the halides using a model hydration shell in section 4.2. Following this is an examination of the intramolecular effects that accompany H-bonding in section 4.3.

As for the heterodimers, we employ electronic structure calculations for the multi-water structures in this section. For the construction of a model hydration shell, several structural choices exist for each anion, $A^- = F^-$, Cl^-, Br^-, and NO_3^-. However, it is desirable to use a common motif that is not only a reasonable, first-order representation of the first aqueous solvation shell of all four anions but also permits, by construction, a direct comparison of the H-bonding characteristics between them. We shall thus not be concerned with obtaining the most stable cluster structure with a given number of H_2O's surrounding the anion; this has already been extensively explored for the halides in several studies.[23,24] We follow a different route, now described.

Six water molecules will be used to make up the model hydration shell of all anions. For the halides, X^-, this shell size is motivated by recent findings of X−H coordination numbers by Soper and Weckström based on neutron scattering experiments.[41] While molecular simulations of aqueous halides using different models have yielded a small spread of coordination numbers,[42] the values are roughly in agreement with experiment.[43] Less is known about the first shell of waters around N O_3^-, with X-ray diffraction[44] and neutron scattering[45] studies suggesting 3−6 and 5 H_2O's, respectively. However, one would intuitively place two waters at each oxygen site of this anion. Recent mixed quantum−classical simulations by Lebrero et al. lend support to this view, indicating an average of 1−3 waters per NO_3^- oxygen.[11] With the view of maximum comparability between properties computed for all four anions, we have chosen the spatial arrangement of waters of Figure 5 as the common structural motif.

An important aspect of this arrangement is that all of the H_2O's are *equivalent*, and the structure has D_{3h} symmetry. We note the omission of water−water H-bonds; these would severely complicate the analysis, and appear not to be critical for the present purposes.[46] Although the chosen motif is obviously very specific and symmetric, some appreciation of its utility comes from the facts that the resulting ordering of the OH red shifts for the anions agrees with the aqueous solution experiments, as (roughly) do the magnitudes (see Table 1).[40] Furthermore, mixed quantum−classical simulations of Tongraar et al. indicate that NO_3^- favors such an arrangement of waters because the distribution of N−O···H angles, though broad, is peaked at an out-of-plane position (around 110°) similar to our choice.[47]

4.2. Reduction of the OH Red Shift for the Anions. We first present an overall comparison of the properties of six-water and one-water complexes of all of the anions. The computed CT-related properties of the former set are listed in the lower half of Table 1. We shall henceforth use N1 as the reference one-water structure for NO_3^-. All six-coordinated anions lose more charge to the waters than in the respective 1:1 complexes. However, this increased extent of total charge transfer is insufficient to overcome its six-part fractionation to the water molecules. Consequently, the charge received per water (q_w) in a given $A^-\cdot 6H_2O$ complex is less than half of its value in the corresponding 1:1 complex, the result applying to the NO_3^- anion as well. The reduced CT, q_w, is reflected in the smaller OH red shifts for the $A^-\cdot 6H_2O$'s compared to that for the one-water complexes, and is consistent with its experimental heterodimer-to-aqueous phase reduction.[17,40,48] Reporting com-

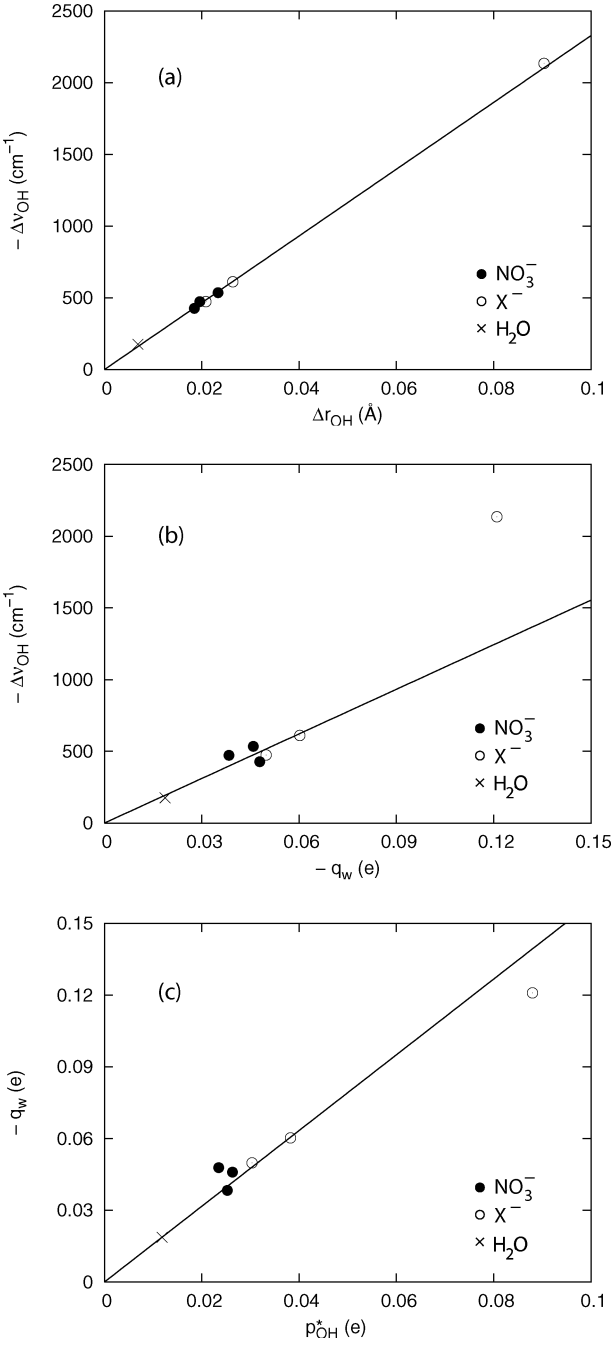

Figure 4. Plots for 1:1 complexes correlating the computed H-bond descriptors, namely, the OH stretch elongation (Δr_{OH}), the charge transferred to the water molecule (q_w), the population in the σ^*_{OH} orbital (p^*_{OH}), and the vibrational red shift of this OH stretch ($\Delta\nu_{OH}$). The three $NO_3^-\cdot H_2O$ complexes are shown with filled circles. The unfilled circles represent the halides, occurring in the order Br^-, Cl^-, and F^- with increasing *x*-coordinate. The water dimer is shown with the ×. The lines represent least-squares linear fits.

putations on halide−water clusters with up to six waters, Kim and co-workers have proffered an argument to the same effect for the red shift trends based on the proton affinity reduction from the bare anion case to when it is H-bonded to several waters.[23,49]

We plot the values of q_w, p^*_{OH}, Δr_{OH}, and $\Delta\nu_{OH}$ against each other in Figure 6, using the data for both one- and six-water complexes (with the exception of $F^-\cdot H_2O$; see section 3.3 and Figure 4). The former set of points is presented with circles (as in Figure 4), and the latter is indicated as squares. For both sets of points, the filled and unfilled shapes are for the nitrate−

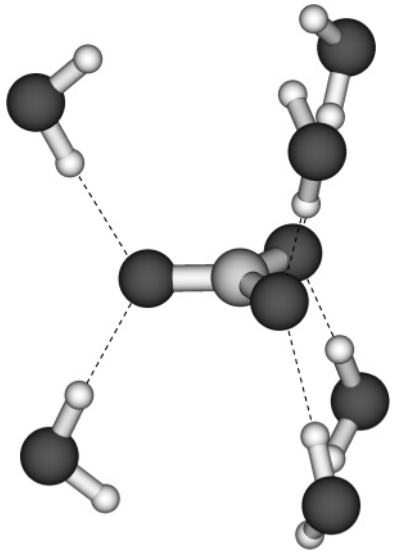

Figure 5. Optimized structure of the $NO_3^-\cdot 6H_2O$ complex having D_{3h} symmetry. The same motif is used for the halide six-water complexes (see section 4.1).

and halide−water complexes, respectively. It is apparent that all of the plotted points fall into the same linear relation; the slopes of the fit lines for this figure and Figure 4 are essentially the same (5−7% difference).

The final comparison we make with the halides is through fractional changes, defined as $f[p] = (p_1 - p_6)/p_1$, p_n being the value of a property in an *n*-water complex. The $f[p]$'s for select properties are shown in Table 2. We find an interesting similarity here between these numbers for the halides and NO_3^-. All of the data in this subsection suggest that, at least for the six-water complex, the NO_3^- anion behaves, loosely speaking, as a large halide.

4.3. Preservation of π-Resonance in NO_3^-. The above results echo the inference drawn in section 4.1 that experimental findings of Bergström et al. indicate that NO_3^- is a weak charge donor toward H-bonding waters.[40] This should be reflected in the absence of charge localization on the anion oxygens. Table 3 lists the Δq's in the $NO_3^-\cdot nH_2O$ structures for $n = 1$, 2, 4, and 6, where an asterisk next to a charge marks a donor oxygen. The two- and four-water structures were derived from Figure 5 with both water molecules next to two and one oxygens removed, respectively.[35] The small changes for the q_O's clearly indicate that the resonance hybrid remains unbroken in all of these nitrate−water complexes. Clearly, π-system preservation is energetically favored over multiple H-bonds in these complexes. The latter continue to act only as a perturbation on the π orbitals, albeit somewhat more strongly than that in the 1:1 complexes. The Δr_{NO} values are in consonance with this statement, the maximum extension being only about 0.025 Å (in the two-water structure). Curiously, for the six-water complex, the NO bonds shorten slightly, and the charges on the O's become less negative by about 0.024*e*.

Although the charge changes in Table 3 are too small for any important charge localization in all of the $NO_3^-\cdot nH_2O$ complexes examined, they do depict a sizable overall charge redistribution effect within the anion, aided by the π-system. Indeed, the largest $|\Delta q_O/q_O^{iso}|$ values (iso = isolated anion) for each case ranges between about 5 and 20%. In addition, the H-bonded oxygens in the 1:1 (N1), 1:2, and 1:4 cases do acquire a larger negative charge relative to the isolated anion ($\Delta q_O <$ 0), while the opposite is true for the non-H-bonded O's. The

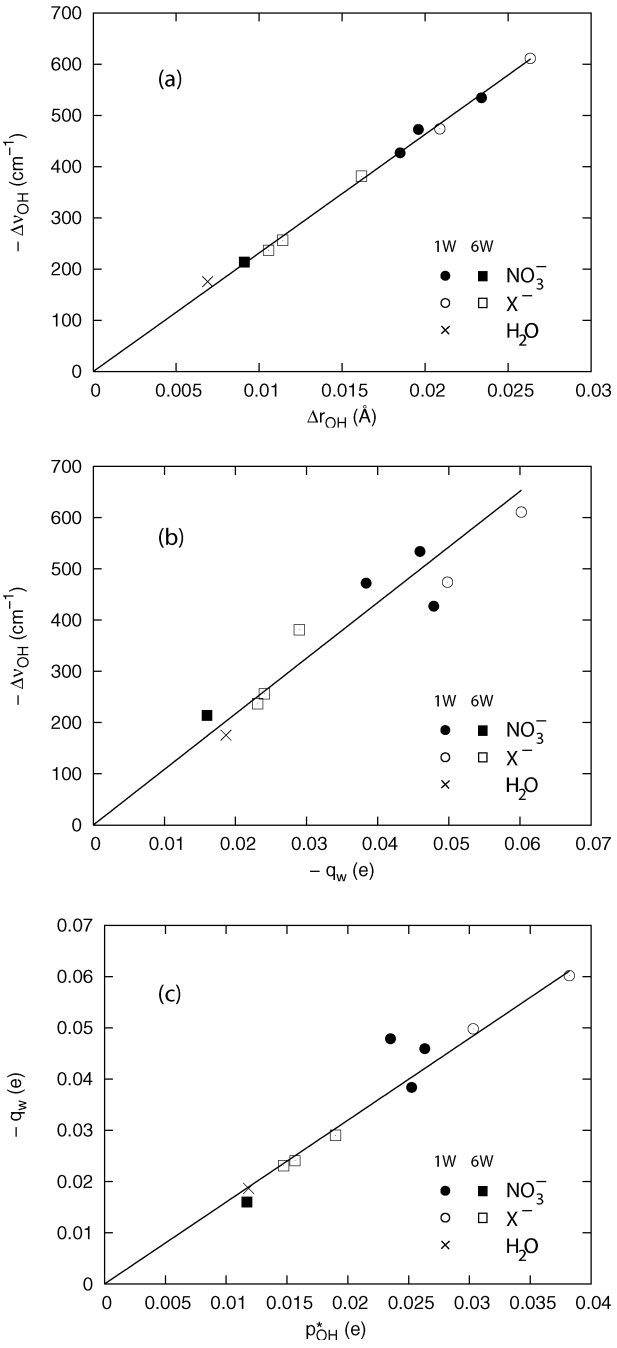

Figure 6. Plots for anion−water $A^-\cdot nH_2O$ complexes, $n = 1$ and 6, correlating the computed H-bond descriptors, namely, the OH stretch elongation (Δr_{OH}), the charge transferred to the water molecule (q_w), the population in the σ^*_{OH} orbital (p^*_{OH}), and the vibrational red shift of this OH stretch ($\Delta\nu_{OH}$). The one-water halide and nitrate complexes are represented as circles, as in Figure 4, while the six-water complexes are shown with squares. In both cases, the filled shapes represent nitrate−water complexes. The × indicates $(H_2O)_2$.

observed net redistribution is a result of both the Coulombic polarization of the anion by the approaching H_2O's and the ensuing CT.[50]

The above observations emphasize the importance of the delocalized valence π-electrons of the planar NO_3^- anion. Such intramolecular effects are expected of other planar ions too, such as CO_3^{2-}. Their magnitudes notwithstanding, the Δq values appear as a sensitive measure of the local environment of NO_3^-, as seen for the two- and four-water cases. They suggest themselves as a possible handle on the symmetry breaking problem in aqueous nitrate solutions referred to in the Introduction.

TABLE 2: Fractional Changes in Select Properties, Namely, the Total Charge on Each Water (q_w) and on the Anion (q_A), and the Population of the σ^*_{OH} Orbital (p^*_{OH}) of the H-Bonded OH Stretch, When the Number of H-Bonded Waters Is Increased from One to Six[a]

	fractional changes		
anion in complex	$f[q_w]$	$f[q_A]$	$f[p^*_{OH}]$
NO_3^-	58%	6%	54%
Br^-	54%	9%	51%
Cl^-	60%	9%	59%
F^-	76%	6%	78%

[a] The columns for a property p are defined as $f[p] = (p_1 - p_6)/p_1$.

TABLE 3: Changes in Natural Charges for the Nitrate Atoms, Relative to the Isolated Anion, for the 1:1 (N1), 1:2, 1:4, and 1:6 $NO_3^-\cdot H_2O$ Complexes[a]

complex	Δq_N	Δq_{O_1}	Δq_{O_2}	Δq_{O_3}	q_w	p^*_{OH}
1:1 (N1)	0.0014	−0.0308 *	0.0339	0.0339	−0.0384	0.0253
1:2	0.0088	−0.0780 *	0.0660	0.0660	−0.0314	0.0222
1:4	0.0179	−0.0220 *	−0.0220 *	0.1132	−0.0218	0.0156
1:6	0.0237	0.0240 *	0.0240 *	0.0240 *	−0.0160	0.0117

[a] The asterisks indicate the H-bonded oxygens. The natural atomic charges for isolated NO_3^- are $q_N = 0.6733e$ and $q_O = -0.5578e$. The charge on each water molecule (q_w) and the population of the antibonding σ^*_{OH} orbital (p^*_{OH}) of the H-bonded OH stretch are also given for each complex.

5. Concluding Remarks

This electronic structure study has focused on the anion−water charge transfer (CT), via the hydrogen (H)-bonds formed between them, for the polyatomic NO_3^- anion and its differences with the monatomic halides, X^- (X = F, Cl, Br). To this end, we have examined one-water and six-water complexes of these anions, the latter being a simple, comparable model of their first aqueous hydration shell in the solution phase. Among the properties calculated for these structures, the red shifts of the frequencies of OH stretches H-bonded to the anions play a significant indicator role. Prior investigations of the halide−water heterodimers have shown that the magnitude of these red shifts are a signature of the efficacy of the CT,[16−19] and the red shifts for all four anions in their aqueous solutions are available for comparison.[40]

The analysis of the one-water structures reveals that NO_3^- is able to carry out about as much charge transfer as Br^-. The data for six-water complexes show that the nitrate anion falls below all of the halides in this respect, a result consistent with the experimental aqueous solution red shift results.[40] Analysis reveals the dominant importance of the delocalizing π-conjugation in NO_3^- compared to the charge localization on the oxygens (which would be preferable for the H-bonded waters), which prevents those O's from acting as three independent H-bonding sites, each with significant negative charge available for CT. In the latter, nonrealized case, CT and OH red shifts would be more important for NO_3^- than for the halides.

In this connection, it would also be of interest to see whether the lack of a loosely bound set of π-electrons, as that for tetrahedral polyatomic anions, leads to notable differences. Preliminary work suggests that this is indeed the case, with ClO_4^- and SO_4^{2-} exhibiting less intramolecular charge redistribution compared to NO_3^- or CO_3^{2-}.[51]

As noted in the Introduction, the nitrate ion is important in various contexts, including atmospheric chemistry[1−8] and in solution,[9−11] and vibrational spectroscopic studies of both the ion and its aqueous environment are important probes of these. That the anion−water CT in aqueous nitrate solution, and hence the measured OH red shift, is low compared to all of the heavy halides corroborates the categorization of NO_3^- as a water "structure breaker". For NO_3^-'s vibrations themselves, the present results should prove relevant for "symmetry breaking", that is, the solvent-induced lowering of symmetry from D_{3h} for the isolated anion, manifested by two distinct bands for the asymmetric NO stretches in aqueous solution, as opposed to a single gas-phase band.[9−11] The splitting occurs even in solutions of low NO_3^- concentration, suggesting that it arises due to an asymmetric aqueous hydration shell.[9,52] Although the overall amount of CT out of NO_3^- is small, the intramolecular charge density appears as a sensitive measure of its local environment, including its asymmetry. Electronic density-based properties could thus prove useful in characterizing such symmetry breaking vibrational signatures, though, clearly, the solvent waters' dynamics must also be taken into account. Reciprocally, this system can be used to enhance the current understanding of water dynamics itself. Owing to the low red shift for the OH stretches H-bonded to it compared to that of even I^-,[14] it allows for an investigation of the OH spectral diffusion at frequencies sufficiently removed from the center of the pure water OH range. Both of these topics are under investigation, in solution as well as at aqueous interfaces, for NO_3^- and for other atmospherically relevant ions such as CO_3^{2-} and SO_4^{2-}.

Acknowledgment. This work was supported in part by ANR Grant NT05-4-43154 and by NSF Grant CHE-0417570.

References and Notes

(1) Solomon, S. *Rev. Geophysics* **1999**, *37*, 275−316.

(2) Bianco, R.; Hynes, J. T. *J. Phys. Chem. A* **1999**, *103*, 3797−3801.

(3) (a) Rivera-Figueroa, A. M.; Sumner, A. L.; Finlayson-Pitts, B. J. *Environ. Sci. Technol.* **2003**, *37*, 548−554. (b) Mochida, M.; Finlayson-Pitts, B. J. *J. Phys. Chem. A* **2000**, *104*, 9705−9711. (c) Saliba, N. A.; Yang, H.; Finlayson-Pitts, B. J. *J. Phys. Chem. A* **2001**, *105*, 10339−10346.

(4) (a) Guimbaud, C.; Arens, F.; Gutzwiller, L.; Gäggeler, H. W.; Ammann, M. *Atmos. Chem. Phys. Discuss.* **2002**, *2*, 739−763. (b) Davies, J. A.; Cox, R. A. *J. Phys. Chem. A* **1998**, *102*, 7631−7642. (c) Beichert, P.; Finlayson-Pitts, B. J. *J. Phys. Chem.* **1996**, *100*, 15218−15228. (d) Ghosal, S.; Hemminger, H. C. *J. Phys. Chem. B* **2004**, *108*, 14102−14108.

(5) (a) Schnitzer, C.; Baldelli, S.; Shultz, M. J. *J. Phys. Chem. B* **2000**, *104*, 585−590. (b) Kido Soule, M. C.; Blower, P. G.; Richmond, G. L. *J. Phys. Chem. A* **2007**, *111*, 3349−3357.

(6) (a) Gibson, E. R.; Hudson, P. K.; Grassian, V. H. *J. Phys. Chem. A* **2006**, *110*, 11785−11799. (b) Hudson, P. K.; Schwarz, J.; Baltursaitis, J.; Gibson, E. R.; Grassian, V. H. *J. Phys. Chem. A* **2007**, *111*, 544−548.

(7) (a) Bianco, R.; Wang, S.; Hynes, J. T. *J. Phys. Chem. A* **2007**, *111*, 11033−11042. (b) Shamay, E. S.; Buch, V.; Parrinello, M.; Richmond, G. L. *J. Am. Chem. Soc.* **2007**, *129*, 12910−12911.

(8) (a) Salvador, P.; Curtis, J. E.; Tobias, D. J.; Jungwirth, P. *Phys. Chem. Chem. Phys.* **2003**, *5*, 3752−3757. (b) Dang, L. X.; Chang, T.-M.; Roeselová, M.; Garrett, B. C.; Tobias, D. J. *J. Chem. Phys.* **2006**, *124*, 066101. (c) Thomas, J. L.; Roeselová, M.; Dang, L. X.; Tobias, D. J. *J. Phys. Chem. A* **2007**, *111*, 3091−3098.

(9) (a) Irish, D. E.; Walrafen, G. E. *J. Chem. Phys.* **1967**, *46*, 378−384. (b) Irish, D. E.; Davis, A. R. *Can. J. Chem.* **1968**, *46*, 943−951. (c) Irish, D. E.; Davis, A. R.; Plane, R. A. *J. Chem. Phys.* **1969**, *50*, 2262−2263. (d) Davis, A. R.; Macklin, J. W.; Plane, R. A. *J. Chem. Phys.* **1969**, *50*, 1478−1479. (e) Chang, T. G.; Irish, D. E. *J. Phys. Chem.* **1973**, *77*, 52−57. (f) Peleg, M. *J. Phys. Chem.* **1972**, *76*, 1019−1025. (g) Lundeen, J. W.; Tobias, R. S. *J. Chem. Phys.* **1975**, *63*, 924−934. (h) Liu, J.-H.; Zhang, Y.-H.; Wang, L.-Y.; Wei, Z.-F. *Spectrochim. Acta, Part A* **2005**, *61*, 893−899.

(10) (a) Waterland, M. R.; Kelley, A. M. *J. Chem. Phys.* **2000**, *113*, 6760−6773. (b) Waterland, M. R.; Stockwell, D.; Kelley, A. M. *J. Chem. Phys.* **2001**, *114*, 6249−6258.

(11) Lebrero, M. C. G.; Bikiel, D. E.; Elola, M. D.; Estrin, D. A.; Roitberg, A. D. *J. Chem. Phys.* **2002**, *117*, 2718−2725.

(12) In principle, the degeneracy of the asymmetric bends ($\nu_4 \approx 700$ cm^{-1}) is also lifted in the aqueous phase. However, the experiments indicate that this splitting becomes noticeable only when the anion concentration is very high, and is considered as a contact ion-pair formation indicator; see, for example, ref 9. Another signature is the appearance of the symmetric NO stretching mode in the IR spectrum, which is only Raman active in the gas phase.

(13) (a) Kropman, M. F.; Bakker, H. J. *J. Chem. Phys.* **2001**, *115*, 8942−8948. (b) Kropman, M. F.; Bakker, H. J. *Science* **2001**, *291*, 2118−2120. (c) Kropman, M. F.; Nienhuys, H.-K.; Bakker, H. J. *Phys. Rev. Lett.* **2002**, *88*, 077601/1−077601/4.

(14) Nigro, B.; Re, S.; Laage, D.; Rey, R.; Hynes, J. T. *J. Phys. Chem. A* **2006**, *110*, 11237−11243.

(15) Laage, D.; Hynes, J. T. *Proc. Natl. Acad. Sci. U.S.A.* **2007**, *104*, 11167−11172.

(16) (a) Ayotte, P.; Weddle, G. H.; Kim, J.; Johnson, M. A. *J. Am. Chem. Soc.* **1998**, *120*, 12361−12362. (b) Ayotte, P.; Kelley, J. A.; Neilsen, S. B.; Johnson, M. A. *Chem. Phys. Lett.* **2000**, *316*, 455−459.

(17) Robertson, W. H.; Johnson, M. A.; Myshakin, E. M.; Jordan, K. D. *J. Phys. Chem. A* **2002**, *106*, 10010−10014.

(18) Roscioli, J. R.; Diken, E. G.; Johnson, M. A.; Horvath, S.; McCoy, A. B. *J. Phys. Chem. A* **2006**, *110*, 4943−4952.

(19) Thompson, W. H.; Hynes, J. T. *J. Am. Chem. Soc.* **2000**, *122*, 6278−6286.

(20) Frisch, M. J.; Trucks, G. W.; Schlegel, H. B.; Scuseria, G. E.; Robb, M. A.; Cheeseman, J. R.; Montgomery, J. A., Jr.; Vreven, T.; Kudin, K. N.; Burant, J. C.; Millam, J. M.; Iyengar, S. S.; Tomasi, J.; Barone, V.; Mennucci, B.; Cossi, M.; Scalmani, G.; Rega, N.; Petersson, G. A.; Nakatsuji, H.; Hada, M.; Ehara, M.; Toyota, K.; Fukuda, R.; Hasegawa, J.; Ishida, M.; Nakajima, T.; Honda, Y.; Kitao, O.; Nakai, H.; Klene, M.; Li, X.; Knox, J. E.; Hratchian, H. P.; Cross, J. B.; Bakken, V.; Adamo, C.; Jaramillo, J.; Gomperts, R.; Stratmann, R. E.; Yazyev, O.; Austin, A. J.; Cammi, R.; Pomelli, C.; Ochterski, J. W.; Ayala, P. Y.; Morokuma, K.; Voth, G. A.; Salvador, P.; Dannenberg, J. J.; Zakrzewski, V. G.; Dapprich, S.; Daniels, A. D.; Strain, M. C.; Farkas, O.; Malick, D. K.; Rabuck, A. D.; Raghavachari, K.; Foresman, J. B.; Ortiz, J. V.; Cui, Q.; Baboul, A. G.; Clifford, S.; Cioslowski, J.; Stefanov, B. B.; Liu, G.; Liashenko, A.; Piskorz, P.; Komaromi, I.; Martin, R. L.; Fox, D. J.; Keith, T.; Al-Laham, M. A.; Peng, C. Y.; Nanayakkara, A.; Challacombe, M.; Gill, P. M. W.; Johnson, B.; Chen, W.; Wong, M. W.; Gonzalez, C.; Pople, J. A. *Gaussian 03*, revision C.02; Gaussian, Inc.: Wallingford, CT, 2004.

(21) (a) Kendall, R. A.; Dunning, T. H., Jr.; Harrison, R. J. *J. Chem. Phys.* **1992**, *96*, 6796−6806. (b) Woon, D. E.; Dunning, Jr., T. H. *J. Chem. Phys.* **1993**, *98*, 1358−1371. (c) Wilson, A. K.; Woon, D. E.; Peterson, K. A.; Dunning, T. H., Jr. *J. Chem. Phys.* **1999**, *110*, 7667−7676.

(22) (a) McCurdy, P. R.; Hess, W. P.; Xantheas, S. S. *J. Phys. Chem. A* **2002**, *106*, 7628−7635. (b) Ramazan, K. A.; Wingen, L. M.; Miller, Y.; Chaban, G. M.; Gerber, R. B.; Xantheas, S. S.; Finlayson-Pitts, B. J. *J. Phys. Chem. A* **2006**, *110*, 6886−6897. (c) Ayotte, P.; Nielsen, S. B.; Weddle, G. H.; Johnson, M. A.; Xantheas, S. S. *J. Phys. Chem. A* **1999**, *103*, 10665−10669.

(23) (a) Kim, J.; Lee, H. M.; Suh, S. B.; Majumdar, D.; Kim, K. S. *J. Chem. Phys.* **2000**, *113*, 5259−5272. (b) Lee, H. M.; Kim, K. S. *J. Chem. Phys.* **2001**, *114*, 4461−4471. (c) Lee, H. M.; Kim, D.; Kim, K. S. *J. Chem. Phys.* **2002**, *116*, 5509−5520.

(24) Wang, X.-B.; Yang, X.; Wang, L.-S.; Nicholas, J. B. *J. Chem. Phys.* **2002**, *116*, 561−570.

(25) (a) Goalwin, P. W.; Kunz, A. B. *Phys. Rev. B* **1987**, *35*, 5795−5801. (b) Pernpointner, M.; Knecht, S. *Chem. Phys. Lett.* **2005**, *419*, 423−429.

(26) Boys, S. F.; Bernardi, F. *Mol. Phys.* **1970**, *19*, 553−566.

(27) (a) Foster, J. P.; Weinhold, F. *J. Am. Chem. Soc.* **1980**, *102*, 7211−7218. (b) Reed, A. E.; Weinstock, R. B.; Weinhold, F. *J. Chem. Phys.* **1985**, *83*, 735−746.

(28) The properties reported in this work have been obtained at the MP2/aug-cc-pVDZ level of theory. The only exceptions are the p^*_{OH} values, which were computed at the RHF level with the same basis.

(29) Colbert, D. T.; Miller, W. H. *J. Chem. Phys.* **1992**, *96*, 1982−1991.

(30) In this connection, we note that MP2 energies were used in the DVR code. In addition, once sufficient ab initio points spanning the desired energy range were obtained, fine-graining of the potential, for the purpose of DVR convergence checks, was done via cubic spline interpolation.

(31) Pimentel, G. C.; McClellan, A. L. *The Hydrogen Bond*; W. H. Freeman and Company: San Francisco, CA, 1960.

(32) Jeffrey, G. A. *An Introduction to Hydrogen Bonding*; Oxford University Press: New York, 1997.

(33) Mulliken, R. S. *J. Phys. Chem.* **1952**, *56*, 801−822.

(34) Though N3 appears to have two H-bonds, only one of the O···HO interactions falls within the standard H-bond geometric limits. The other one has too large an O···H distance (≈2.4 Å), and its OHO angle is much

too bent (≈122°). Furthermore, the σ^*_{OH} population for this OH stretch is only a tenth of that for the H-bonded OH.

(35) Optimizations for all structures were carried out with dihedral constraints alone, which preserved the plane of the H_2O molecules and, hence, the symmetry set for the initial structure. All other degrees of freedom were allowed to freely adjust.

(36) Ebner, C.; Sansone, R.; Probst, M. *Int. J. Quantum Chem.* **1998**, *70*, 877−886.

(37) The motion corresponding to the imaginary frequency in N1 is the outer OH wag about the H-bond axis.

(38) *NIST Standard Reference Database Number 69*; National Institute of Standards and Technology: Gaithersburg, MD, 2005.

(39) By the same reasoning, an oxygen atom with a localized full (or nearly full) negative charge and unfettered by π-delocalization should be able to effect a strong CT. Roscioli et al. (ref 18) discuss the extreme example of OH^-, which exhibits a dramatically large OH red shift in its one-water complex.

(40) Bergström, P. A.; Lindgren, J.; Kristiannson, O. *J. Phys. Chem.* **1991**, *95*, 8575−8580.

(41) Soper, A. K.; Weckström, K. *Biophys. Chem.* **2006**, *124*, 180−191.

(42) (a) Koneshan, S.; Rasaiah, J. C.; Lynden-Bell, R. M.; Lee, S. H. *J. Phys. Chem. B* **1998**, *102*, 4193−4204. (b) Heuft, J. M.; Meijer, E. J. *J. Chem. Phys.* **2003**, *119*, 11788−11791.

(43) The simulations for the halide ions X^- often report the X−O coordination number in the approximate range of 5−7. This number is expected to be slightly larger than its X−H counterpart based on neutron diffraction measurements, such as ref 41.

(44) Caminiti, R.; Licheri, G.; Paschina, G.; Piccaluga, G.; Pinna, G. *J. Chem. Phys.* **1980**, *72*, 4522−4528.

(45) Kameda, Y.; Saitoh, H.; Uemura, O. *Bull. Chem. Soc. Jpn*. **1993**, *66*, 1919−1923.

(46) One expects numerous intermolecular water−water H-bonds in the immediate vicinity of the studied anions in the solution phase. In the present anion−water CT context, such H-bonds will likely introduce difficulties into the interpretation of results owing to the cooperativity effect; see, for example, ref 32. On the other hand, such H-bond structures can induce an asymmetric local environment around an anion, an aspect of particular relevance to NO_3^- in solution in connection with "symmetry breaking".

(47) Tongraar, A.; Tangkawanwanit, P.; Rode, B. M. *J. Phys. Chem. A* **2006**, *110*, 12918−12926.

(48) In addition to the red shifts in Table 1, the reduced CT q_w is also reflected in an increase in the (A_d−O_w) distances, A_d being the anion donor site. Thompson and Hynes have shown that the anion−water separation is an important factor in determining the extent of CT and related effects for $X^-\cdot H_2O$ (ref 19); for example, it is key for the large CT in $F^-\cdot H_2O$. The Table 1 data extend their reasoning to larger clusters, providing a measure of sensitivity of the H-bond properties to the $r(A_d-O_w)$ changes.

(49) Kim and coworkers employed halide−water clusters with up to six waters, chosen based on their stability for a given number (n) of waters (ref 23). Several structures contain H_2O-H_2O H-bonds, which we have avoided in the present work. Owing to the "surface-like" ion location in these clusters, the number of H_2O's directly H-bonded to the halide is less than n in some cases, particularly for $n = 5, 6$. Thus, while the anion increasingly loses charge to surrounding waters as their count increases, it is clearly not split into n parts. The CT and the resulting OH red shift are strongly dependent on the structure, and detailed comparison is difficult.

(50) It is important to make a distinction between these two stages, particularly as regards the role of the non-H-bonded oxygens in the overall process. While it *appears* as if they take on the CT burden, much of the Δq on them may arise from the Coulombic polarization stage itself.

(51) Re, S.; Ramesh, S. G.; Hynes, J. T. Unpublished.

(52) (a) Gertner, B. J.; Ando, K.; Bianco, R.; Hynes, J. T. *Chem. Phys.* **1994**, *183*, 309−323. (b) Benjamin, I.; Barbara, P.; Gertner, B. J.; Hynes, J. T. *J. Phys. Chem.* **1995**, *99*, 7557−7567. (c) Sato, H.; Hirata, F.; Myers, A. B. *J. Phys. Chem. A* **1998**, *102*, 2065−2071. (d) Zhang, F. S.; Lynden-Bell, R. M. *Phys. Rev. Lett*. **2003**, *90*, 185505/1−185505/4. (e) Sanov, A.; Lineberger, W. C. *Phys. Chem. Commun.* **2002**, *5*, 165−177.

(53) Multiple values for the proton affinity of NO_3^- are listed in the NIST database (ref 38). For Figure 3, we have used a rough average value of 1370 kJ/mol.